Conditional moments of the breakthrough curves of kinetically sorbing solute in heterogeneous porous media using multirate mass transfer models for sorption and desorption

Alison E. Lawrence

Department of Civil and Environmental Engineering, University of California, Berkeley, California, USA

Xavier Sanchez-Vila

Department of Geotechnical Engineering and Geosciences, Technical University of Catalonia, Barcelona, Spain

Yoram Rubin

Department of Civil and Environmental Engineering, University of California, Berkeley, California, USA

Received 12 October 2001; revised 24 May 2002; accepted 24 May 2002; published 21 November 2002.

[1] A methodology is presented for evaluating the temporal moments of solutes undergoing linear rate-limited mass transfer processes based on a Lagrangian approach to solute transport in heterogeneous media. The temporal moments of sorbing solutes are written as a function of those of conservative tracers. The general continuous diffusion rate model that has recently appeared in the hydrologic literature is used to model the rate-limited mass transfer processes. The methodology is also applied to desorption from an initially uniformly contaminated aquifer, and the concentration expected value and variance are found quasi-analytically. The conditional temporal moments of sorbing solutes can be written as a function of the conditional moments of conservative tracers. Conditioning results in a reduction of the variance of travel time. The amount of reduction depends on the chemical model selected. *INDEX TERMS:* 1829 Hydrology: Groundwater hydrology; 1832 Hydrology: Groundwater transport; 1869 Hydrology: Stochastic processes; 1831 Hydrology: Groundwater hydrology; *KEYWORDS:* reactive transport, temporal moments, groundwater, conditional statistical moments, multirate sorption, desorption

Citation: Lawrence, A. E., X. Sanchez-Vila, and Y. Rubin, Conditional moments of the breakthrough curves of kinetically sorbing solute in heterogeneous porous media using multirate mass transfer models for sorption and desorption, *Water Resour. Res.*, *38*(11), 1248, doi:10.1029/2001WR001006, 2002.

1. Introduction

[2] The subject of evaluating temporal moments to a control plane for conservative and reactive tracers in heterogeneous media has been receiving increasing attention in the groundwater literature since the late 1980s. A possible explanation is the awareness that most of the information that can be gathered in the field is in the form of breakthrough curves (BTCs). Another important reason is that most environmental regulations are based upon probabilities of not exceeding a given concentration in a predetermined amount of time (mass flux arrival times).

[3] Temporal moments in heterogeneous domains are usually analyzed within a Lagrangian framework, where the travel time, τ, is the time for a particle to move from its initial location to a control plane. τ is not known deterministically due to the impossibility of fully sampling the heterogeneous domain, so it is treated as a random variable and the low-order moments are derived.

[4] Past work on conservative tracers has determined the moments of the travel time for different domain dimensionalities, different correlation models, and different flow configurations. Most of the studies consider uniform mean flow. Initial work, by *Shapiro and Cvetkovic* [1988], provided the temporal moments for long travel distances. *Cvetkovic et al.* [1992] obtained the first two moments for travel time as a function of distance in isotropic 2-D and 3-D correlation models. *Bellin et al.* [1992] numerically obtained travel time cumulative distribution functions (CDFs). *Rubin and Dagan* [1992] presented a method to condition the travel time CDF on transmissivity measurements. *Sanchez-Vila* [1995] derived analytical expressions for the 2-D isotropic case including local dispersion. *Cvetkovic et al.* [1996] provided analytical-numerical results for the first two temporal moments, showing dependence of the mean of τ on distance. Nonlinearity of the mean of τ, which affects the results for second order in τ, had not been considered in the previous analytical approaches. Finally, *Dagan and Indelman* [1999] developed the temporal moments for the dipole flow case.

[5] The study of temporal moments of sorbing solutes has been carried out in parallel. In most of the literature, the sorption models considered are either instantaneous equilibrium or one-site kinetics [e.g., *Cvetkovic and Shapiro*, 1990; *Selroos and Cvetkovic*, 1992]. *Harvey and Gorelick* [1995] derived differential equations for the temporal moments of kinetically sorbing solutes for instantaneous equilibrium, first order kinetics, and the mobile-immobile

0043-1397/02/2001WR001006

domain model. These equations take the form of the nonreactive transport equation with different source terms, so that they may be solved using any existing code that can solve the nonreactive transport equation. *Valocchi* [1985] and *Goltz and Roberts* [1987] derived equations for the temporal moments of a solute undergoing linear kinetic sorption in a homogeneous hydraulic conductivity field. *Rubin et al.* [1997] developed a general methodology that could be applied to the two-site kinetics model and the mobile-immobile domain model and that could include conditioning in a straightforward manner. Conditioning ensures that measured values, such as values of hydraulic conductivity, are fully utilized. *James et al.* [1997] presented a method for conditioning the temporal moments of a solute retarded by local equilibrium sorption. *Cvetkovic et al.* [1998] provided a general framework to incorporate other types of linear nonequilibrium sorption processes with variability in the sorption parameters. *Cvetkovic et al.* [1999] extended their previous results to incorporate matrix diffusion. For a detailed explanation of the sorption process, see *Grathwohl* [1998].

[6] In the last few years, the hydrologic literature has focused on new, more general, mass transfer models that recognize the possibility of having a large number of mass transfer rates between water and soil at any single location. The initial models are termed multirate discrete models [*Haggerty and Gorelick*, 1995; *Chen and Wagenet*, 1995]. An immediate extension is a model that assumes a continuous distribution of mass transfer rates [*Chen and Wagenet*, 1995; *Haggerty and Gorelick*, 1998]. The continuous model had previously been used effectively in the soil contamination literature [e.g., *Connaughton et al.*, 1993; *Pedit and Miller*, 1994] for interpreting desorption experiments in laboratory columns, which shows the potential of this model. Subsequently, many authors have investigated the efficiency of different continuous models. There has been some agreement that the gamma and the lognormal models (to be presented later in this paper) are the ones that provide the best fit to experimental results [*Culver et al.*, 1997; *Haggerty and Gorelick*, 1998; *Deitsch et al.*, 2000].

[7] In order to focus on the effect of multirate mass transfer on solute transport, we treat the parameters for the sorption models as spatially uniform but treat hydraulic conductivity as variable in space, as has been done in several other studies [*Berglund and Cvetkovic*, 1995; *Selroos*, 1995; *Rubin et al.*, 1997; *Dagan and Indelman*, 1999]. Therefore our results are valid for aquifers in which the sorption parameters vary only slightly in space. In this paper, we extend the formulation of *Rubin et al.* [1997] to incorporate a continuous distribution of mass transfer rate coefficients. We find that the moments of the BTC for a sorbing solute can be written in terms of those for a conservative one. Closed form expressions for the temporal moments are obtained for the three continuous distribution models most commonly used in the literature: two-site kinetics, gamma, and lognormal. In addition, we show how conditioning can be incorporated into the method.

2. Mathematical Statement of the Problem

[8] The problem can be stated as finding the moments of the travel time for a sorbing solute traveling from an injection point to a control plane downgradient under any given flow conditions. To reach the control plane, the solute follows a certain streamtube, which will be tortuous due to heterogeneity. Along this streamtube, it is possible to write the advection-dispersion equation in dimensionless form [see, e.g., *Haggerty and Gorelick*, 1995; *Rubin et al.*, 1997; *Rubin*, 2002, chap. 10]:

$$\frac{\partial C_1}{\partial T} + \beta_{tot}\frac{\partial C_2}{\partial T} + V\frac{\partial C_1}{\partial \eta} = 0, \tag{1}$$

where C_1 is the dimensionless mobile concentration ($C_1 = C'_1/C_{1,ref}$, where C'_1 is mobile solute mass per unit volume of fluid, and $C_{1,ref}$ is a reference concentration); C_2 is the dimensionless immobile concentration ($C_2 = C'_2/(K_D C_{1,ref})$, where C'_2 is sorbed mass per unit mass of soil, and K_D is the distribution coefficient); V is dimensionless velocity ($V = v/U$, where v is the actual velocity, and U is a reference velocity); T is dimensionless time ($T = Ut/I_Y$, where t is actual time, and I_Y is the integral scale of the log hydraulic conductivity, Y, in the mean flow direction); and η is the coordinate along the streamtube, nondimensionalized by I_Y. The parameter β_{tot} is the total capacity factor, which has been nondimensionalized by multiplication with K_D. The total capacity factor is the ratio of the total mass in the immobile zone to the total mass in the mobile zone at equilibrium [*Haggerty and Gorelick*, 1998]. For example, when porosity in the immobile zone is neglected, $\beta_{tot} = \rho_s K_D(1 - \phi)/\phi$, where ϕ is the porosity of the mobile zone and ρ_s is the mass density of the soil solids. In (1), local dispersion has been neglected, so that no mass transfer between streamtubes is considered. Equation (1) must be coupled with an equation describing the kinetics of the mass transfer process.

[9] The equations for the mass transfer model with a continuous distribution of mass transfer rate coefficients are [*Haggerty and Gorelick*, 1998]

$$\frac{\partial C_1}{\partial T} + \int_0^\infty \beta(\alpha)\frac{\partial C_2(\alpha)}{\partial T}\,d\alpha + V\frac{\partial C_1}{\partial \eta} = 0, \tag{2}$$

$$\frac{\partial C_2(\alpha)}{\partial T} = \alpha[C_1 - C_2(a)], \tag{3}$$

where α is a dimensionless mass transfer rate coefficient ($\alpha = \alpha' I_Y/U$, where α' is the mass transfer rate coefficient with units 1/time). Therefore it is explicitly stated in (2) and (3) that the concentration in the immobile domain is not represented by a single value, but by a continuous distribution of values. *Haggerty and Gorelick* [1998] discuss the convenience of writing $\beta(\alpha)$ in terms of the total capacity factor, $\beta_{tot} = \int_0^\infty \beta(\alpha)d\alpha$; therefore $\beta(\alpha)$ can be written the following way:

$$\beta(\alpha) = \beta_{tot}\ p(\alpha), \tag{4}$$

where $p(\alpha)$ can be any function such that $p(\alpha)$ is nonnegative and real for all nonnegative and real values of α, and $\int_0^\infty p(\alpha)d\alpha = 1$.

3. General Solution

[10] The problem considered is a pulse of concentration instantaneously injected at time zero into a clean aquifer, so that the initial and boundary conditions are

$$C_1(\eta, T = 0) = C_2(\eta, T = 0) = 0, \tag{5}$$

$$C_1(\eta \to \infty, T) = 0 \tag{6}$$

and

$$C_1(\eta = 0, T) = \delta(T). \tag{7}$$

Applying the Laplace transform to the coupled equations (2) and (3) gives

$$\begin{aligned} s\overline{C}_1 + s\int_0^\infty \beta(\alpha)\overline{C}_2(\alpha)d\alpha &= -V\frac{\partial \overline{C}_1}{\partial \eta}, \\ s\overline{C}_2(\alpha) &= \alpha\left[\overline{C}_1 - \overline{C}_2(\alpha)\right], \end{aligned} \tag{8}$$

where an overbar on a variable indicates the Laplace transform of the variable. Equations (8) can be combined to form a single equation for $\overline{C}_1$:

$$s\overline{C}_1\left(1 + \int_0^\infty \frac{\alpha}{s+\alpha}\beta(\alpha)d\alpha\right) = -V\frac{\partial \overline{C}_1}{\partial \eta}. \tag{9}$$

We now let L represent the Euclidean distance along the mean trajectory from the source to the control point or plane. The solution of (9) for this case is

$$\overline{C}_1(L, s) = \exp\left[-s\tau(L)\left(1 + \beta_{tot}\int_0^\infty \frac{\alpha}{s+\alpha}p(\alpha)d\alpha\right)\right], \tag{10}$$

where τ, given by

$$\tau(L) = \int_0^{\eta(L)} \frac{d\eta'}{V(\eta')}, \tag{11}$$

corresponds to the travel time along the trajectory from the injection point (η = 0) to the control plane located at the Euclidian distance L, or at a distance η(L) along the trajectory, downstream. In a real medium, L will be known, but η will not.

[11] As the medium is heterogeneous, no explicit results for τ(L) can be obtained for any given domain or flow configuration, unless the domain is sampled exhaustively. An alternative is to work with the expected BTC. Usually, the stochastic variable in flow problems is hydraulic conductivity (3-D analysis) or transmissivity (2-D analysis). In this approach, τ(L) is considered a random variable, and we can substitute information about its statistical moments for its unknown actual value.

[12] As (10) is valid in any given realization of the heterogeneous domain, the mean concentration in Laplace space is simply found by taking the ensemble average of (10) over τ:

$$\langle\overline{C}_1(L, s)\rangle = \langle\exp\left[-s\tau\left(1 + \beta_{tot}\int_0^\infty \frac{\alpha}{s+\alpha}p(\alpha)d\alpha\right)\right]\rangle. \tag{12}$$

The noncentral temporal moments of the expected BTC, which are given by

$$T_i^R(L) = \frac{\int_0^\infty t^i\langle C_1(L, t)\rangle dt}{\int_0^\infty \langle C_1(L, t)\rangle dt}, \tag{13}$$

can be computed directly from (10) without having to determine the expression for C_1 in real space using the result of *Aris* [1958]: $t_i(L) = (-1)^i d^i/ds^i|_{s=0}$ where $t_i(L) = \int_0^\infty t^i dt$. Using this relationship, the first, second, and third central moments of the travel time are

$$\langle\tau^R\rangle = T_1^R = (1 + \beta_{tot})\langle\tau^{NR}\rangle, \tag{14}$$

$$\sigma_\tau^{2,R} = T_2^R - \left(T_1^R\right)^2 = \sigma_\tau^{2,NR}(1 + \beta_{tot})^2 + 2\beta_{tot}\int_0^\infty \frac{p(\alpha)}{\alpha}d\alpha, \tag{15}$$

$$\begin{aligned} \Sigma_\tau^R &= T_3^R - 3T_1^R T_2^R + 2\left(T_1^R\right)^3 \\ &= \Sigma_\tau^{NR}(1 + \beta_{tot})^3 + 6\sigma_\tau^{2,NR}\beta_{tot}(1 + \beta_{tot}) \\ &\quad \int_0^\infty \frac{p(\alpha)}{\alpha}d\alpha + 6\langle\tau^{NR}\rangle\beta_{tot}\int_0^\infty \frac{p(\alpha)}{\alpha^2}d\alpha, \end{aligned} \tag{16}$$

where the dependence on L is not shown, for brevity. The superscripts R and NR stand for reactive and nonreactive solutes respectively. Notice that the mathematical expressions do not depend on the flow configuration or the dimensionality of the problem, and that these appear implicitly in τ^{NR}. The method is easily extended to higher-order moments. Equations (14)–(16) give the statistical moments of the breakthrough curve for a reactive solute as a function of those of a conservative tracer. These are ensemble moments for one streamtube. When the domain is stationary, they are equivalent to moments over many streamtubes at the control plane in one realization for a line of injection that is long in a direction normal to the mean flow direction. The parameters defining the chemical model are assumed uniform. The general solution given here can be specialized to the desired model by using the appropriate p(α).

[13] The temporal moments for conservative tracers that appear in (14)–(16) can be obtained from the relationships between central and noncentral moments and the CDF of τ, G(L, τ) [see *Rubin et al.*, 1997]:

$$= \int_0^\infty i\tau^{i-1}(1 - G(L, \tau))d\tau. \tag{17}$$

The expression for G(L, τ) for transport of a conservative tracer to a control plane normal to the mean flow direction is given by *Dagan and Nguyen* [1989]. For the specific case of a Gaussian pdf for displacements, the expression becomes [*Dagan and Nguyen*, 1989]

$$G(L, \tau) = \frac{1}{2}\mathrm{erfc}\left(\frac{L - \langle X_1(\tau)\rangle}{\sqrt{2X_{11}(\tau)}}\right), \tag{18}$$

where $X_{11}(\tau)$ is the longitudinal solute displacement variance at time τ, and $X_1(\tau)$ is the longitudinal displace-

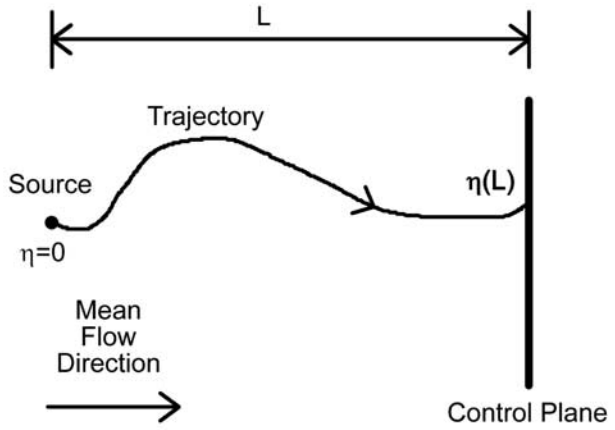

Figure 1. Definition sketch showing one possible path that the solute would travel to the control plane. The travel time is the time it takes the solute to travel from the source to the control plane.

ment at time τ. For the case of uniform in the average flow, the situation is shown in Figure 1.

4. Commonly Used Models

[14] The models investigated in the following sections, which have been used extensively in the literature for linear mass transfer rate-limited processes, are the one-site kinetic model, the two-site kinetics model, the gamma model, and the lognormal model. For a single sorption site, the continuous model for $\beta(\alpha)$ reduces to $\beta(\alpha) = \beta_{tot}\delta(\alpha - \alpha_1)$, and (1) is immediately recovered from (2). Therefore for the one-site model, $p(\alpha)$ is the Dirac delta function: $p(\alpha) = \delta(\alpha - \alpha_1)$.

[15] In a multirate discrete model, $p(\alpha)$ is given by multiple spikes corresponding to the different rates considered in the model: $p(\alpha) = \sum_{i=1}^{N}(\beta_i/\beta_{tot})\delta(\alpha - \alpha_i)$, where N is the finite number of spikes. A discrete multirate model with two mass transfer rates is referred to as the two-site kinetics model. Each of the two different reaction rates employed in the two-site kinetics model is associated with a volumetric fraction of the sorption sites. The expression for $p(\alpha)$ is given by a function with two singularities:

$$p(\alpha) = \frac{\beta_1}{\beta_{tot}}\delta(\alpha - \alpha_1) + \frac{\beta_2}{\beta_{tot}}\delta(\alpha - \alpha_2). \tag{19}$$

If $\alpha_1 \cong \alpha_2$, the one-site kinetic model is recovered, with $\beta_{tot} = \beta_1 + \beta_2$. However, there is usually a difference in orders of magnitude between α_1 and α_2, as they can be associated with different particle sizes (e.g., clays and silts). When $\alpha_2 \gg \alpha_1$ and $\alpha_2 \to \infty$, the soil fraction corresponding to β_2 can be considered to be in instantaneous equilibrium, and the mobile-immobile domain model [*van Genuchten and Wierenga*, 1976] is recovered. The two-site model used in this way is often referred to as the equilibrium/kinetic two-site model. Although the distributed rate parameter models (such as lognormal and gamma) often provide a better fit than the two-site model, there are some cases where the two-site model performs better. For example, *Haggerty and Gorelick* [1998] found that for one desorption case of TCE from sand from Livermore, California, a model with two rate coefficients performed better than the gamma and lognormal models. In addition, *Culver et al.* [1997] found that the two-site equilibrium/kinetic model best fits desorption data when the time of exposure to the contaminant was small (1 week for a laboratory-scale experiment). *Karapanagioti et al.* [1999] found that introducing a second rate to model fast sorption improved the match to experimental data for phenanthrene sorption to an alluvial aquifer material compared to using a single rate.

[16] In a continuous model, $p(\alpha)$ can be any piecewise continuous function with unit integral. The gamma model may be the most commonly used continuous model in the literature [*Connaughton et al.*, 1993; *Pedit and Miller*, 1994; *Chen and Wagenet*, 1995; *Culver et al.*, 1997; *Deitsch et al.*, 2000]. The gamma model has two positive parameters, which are the shape parameter, a, and the scale parameter, b. The expression for $p(\alpha)$ is

$$p(\alpha) = \frac{\alpha^{a-1}}{b^a\Gamma(a)}\exp\left(-\frac{\alpha}{b}\right). \tag{20}$$

The gamma model is very flexible, as can be seen by examining the shape of $p(\alpha)$ for different values of the shape parameter, a, in Figure 2. $p(\alpha)$ for this model can range from an exponential distribution to a normal distribution.

[17] The lognormal model is the other most commonly used distribution for distributed mass transfer rate coefficients. The lognormal model is based on physical considerations, as grain size usually follows a lognormal distribution, and rate coefficients are linked to grain size [*Buchan et al.*, 1993]. This model has been successfully used to interpret BTCs in desorption experiments by *Pedit and Miller* [1994] and *Haggerty and Gorelick* [1998], and more recently, has been successfully applied to the interpretation of single-well and convergent flow tracer tests at the Waste Isolation Pilot Plant site in New Mexico [*Haggerty et al.*, 2001; *McKenna et al.*, 2001]. Like the gamma model, the lognormal model is a two-parameter model. The two parameters correspond to the mean, μ, and the standard deviation, σ, of the natural logarithm of the mass transfer rate coefficients, α. The expression for $p(\alpha)$ is

$$p(\alpha) = \frac{1}{\sqrt{2\pi}\sigma\alpha}\exp\left[-\frac{1}{2\sigma^2}(\ln\alpha - \mu)^2\right]. \tag{21}$$

5. Application to One and Two Mass Transfer Rates

[18] In the one-site kinetic model, $\beta(\alpha) = \beta_{tot}\delta(\alpha - \alpha_1)$, so that

$$\langle C_1(L,s)\rangle = \langle\exp\left[-s\tau(L)\left(1 + \beta_{tot}\frac{\alpha_1}{s + \alpha_1}\right)\right]\rangle. \tag{22}$$

Therefore

$$\langle\tau^R(L)\rangle = (1 + \beta_{tot})\langle\tau^{NR}(L)\rangle, \tag{23}$$

$$\sigma_\tau^{2,R}(L) = \sigma_\tau^{2,NR}(L)(1 + \beta_{tot})^2 + 2\frac{\beta_{tot}}{\alpha_1}\langle\tau^{NR}(L)\rangle, \tag{24}$$

$$\Sigma_\tau^R(L) = \Sigma_\tau^{NR}(L)(1 + \beta_{tot})^3 + 6\sigma_\tau^{2,NR}(L)\frac{\beta_{tot}}{\alpha_1}(1 + \beta_{tot}) + 6\frac{\beta_{tot}}{\alpha_1^2}\langle\tau^{NR}(L)\rangle. \tag{25}$$

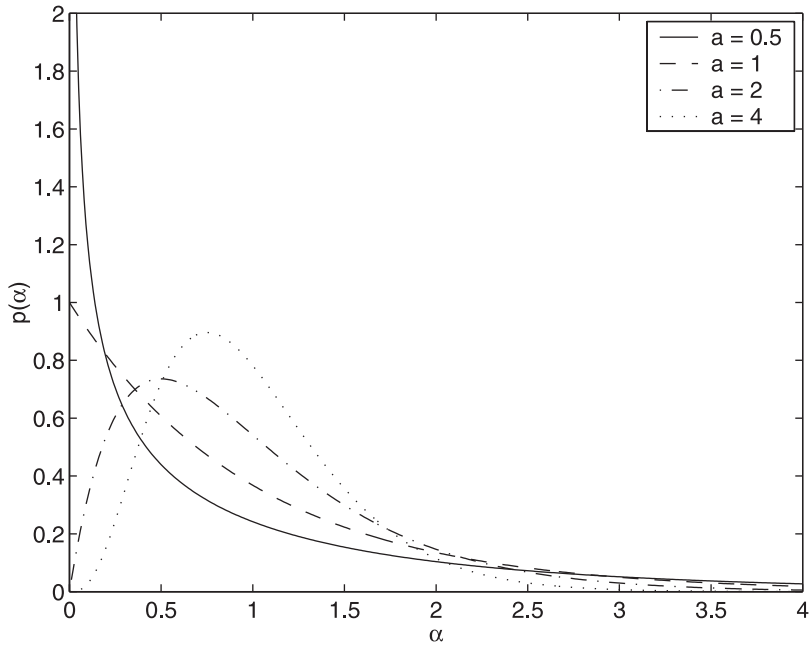

Figure 2. Probability density functions for the gamma distribution for different values of the shape parameter, a.

Closed form expressions for equations (23), (24), and (25) can be obtained using (18) to determine G(L, τ).

[19] For the two-site kinetics model, the first moment is still given by (23), while the second moment becomes

$$\sigma_\tau^{2,\mathrm{R}}(\mathrm{L}) = \sigma_\tau^{2,\mathrm{NR}}(\mathrm{L})(1+\beta_{\mathrm{tot}})^2 + 2\left(\frac{\beta_1}{\alpha_1}+\frac{\beta_2}{\alpha_2}\right)\langle\tau^{\mathrm{NR}}(\mathrm{L})\rangle. \quad (26)$$

[20] To evaluate the impact of the chemical parameters on the second moment, we compare with the second temporal moment for a conservative tracer. Combining (17), (18), and X_{11} from *Dagan* [1989, equation 4.6.14] for three-dimensional, uniform in the average flow with an isotropic exponential log hydraulic conductivity covariance, we obtain the expressions for the nonreactive temporal moments. The integration is performed numerically. In the subsequent analysis, we concentrate on the ratio of the variance of the travel time to a control plane a distance L downstream for a reactive solute to that of a conservative solute, which, from (26), is given by

$$\frac{\sigma_\tau^{2,\mathrm{R}}(\mathrm{L})}{\sigma_\tau^{2,\mathrm{NR}}(L)} = (1+\beta_{\mathrm{tot}})^2 + 2\left(\frac{\beta_1}{\alpha_1}+\frac{\beta_2}{\alpha_2}\right)\frac{}{\sigma_\tau^{2,\mathrm{NR}}(\mathrm{L})}. \quad (27)$$

For any given choice of chemical parameters, the variance ratio is a monotonically decreasing function that goes from infinity at L $\rightarrow$ 0 to a constant value for large travel distances. The travel time variance curves for the geochemical models with a continuous distribution of mass transfer rates also take this shape. This is due to the effect of sorption. At very early times, only some of the solute has been sorbed, and some has acted as a nonreactive tracer. Therefore the spread between the portion that has been retarded and the portion that has not is large compared to the spread of a nonreactive tracer. This larger spread is indicated by the large travel time variance ratio. As time increases, more of the solute experiences sorption and the resulting retardation, which partially counteracts the spreading, and the variance ratio begins to decrease. The variance ratio (27) consists of two terms, one depending on β_{tot} and one depending on all of the reaction parameters and the expected value of the nonreactive travel time. The term that causes the variance ratio to decrease at early times is the second term, which decreases when $\sigma_\tau^{2,\mathrm{NR}}$ grows faster than $\langle\tau^{\mathrm{NR}}\rangle$.

[21] The next step is to find the sensitivity of (27) to the different parameters involved in the formulation. The parameters for the geochemical model are varied over the general ranges over which they have been found to vary in the experiments by *Haggerty and Gorelick* [1998] and *Culver et al.* [1997]. Figure 3 shows the variance ratio versus distance for different values of β_1, while β_{tot}, and therefore the first moment (see equation 23), remain constant. Notice that the variance ratio in (27) decreases as β_1 decreases, provided $\alpha_2 \gg \alpha_1$. This occurs because as β_1 decreases, fewer of the sorption sites are associated with the smaller rate coefficient, α_1. The rapid rate, α_2, dominates, so the effects of nonequilibrium sorption are reduced. For very small values of β_1, the variance ratio curves are very close to each other. Physically, this is because going from $\beta_1 = 0.1$ to $\beta_1 = 0.01$ is equivalent to going from 0.1% to 0.01% of the sorption sites being governed by α_1, because β_{tot} is 100. This is a very small change in the actual number of sites associated with α_1. In a similar analysis, by varying α_1 while β_1, β_2 and the alpha ratio (α_1/α_2) remain constant, we found that the variance ratio decreases as α_1 increases.

6. Application to a Continuous Distribution of Mass Transfer Rates

6.1. Gamma Model for p(α)

[22] For the gamma model, given by (20), the expression for $\langle C_1\rangle$ in Laplace space is

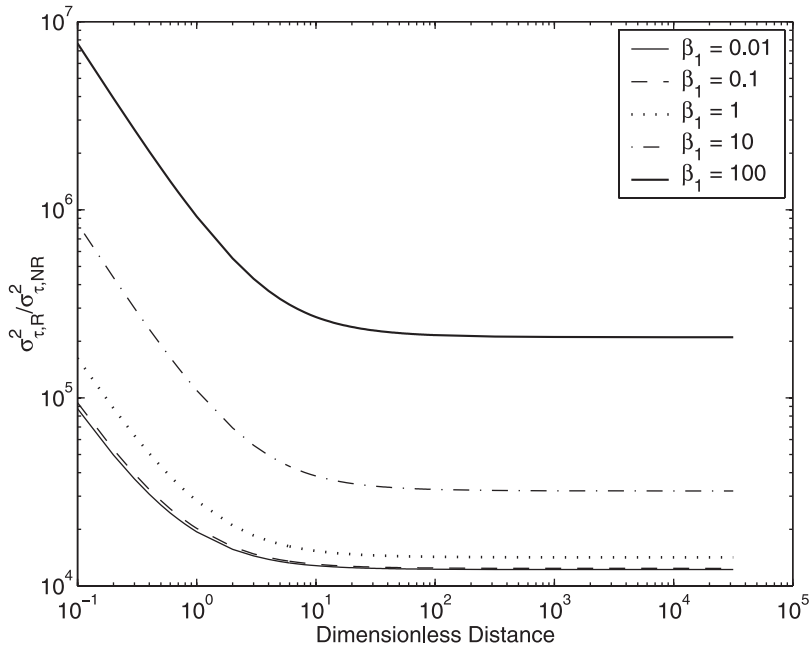

Figure 3. Impact of β_1 (while keeping β_{tot} constant) in the two-site model upon the ratio between the variance of travel time for a reactive solute with respect to that of a nonreactive solute as a function of distance in an unbounded three-dimensional domain under uniform mean flow conditions. The additional parameters remain constant: $\beta_{tot} = 100$, $\alpha_1 = 0.001$, $\alpha_2 = 0.1$ and $\alpha_Y{}^2 = 0.5$.

$$\langle \overline{C}_1(L,s)\rangle = \langle \exp\Big\{-st(L)\Big[1+ab_{tot}\Big(\frac{s}{b}\Big)^a \cdot \exp(s/b)\Gamma(-a,s/b)\Big]\Big\}\rangle, \quad (28)$$

where $\Gamma(-a, s/b)$ is the incomplete gamma function, defined as

$$\Gamma\Big(-a,\frac{s}{b}\Big) = \int_{s/b}^{\infty} \frac{\exp(-t)}{t^{a+1}}dt. \quad (29)$$

[23] In a few cases in the literature, the best fit to the lab or field concentration curves were obtained with a very large value of a ($a \gg 1$) [*Culver et al.*, 1997; *Deitsch et al.*, 2000]. In most cases, $a < 1$ [*Connaughton et al.*, 1993; *Pedit and Miller*, 1994; *Culver et al.*, 1997; *Deitsch et al.*, 2000], which means that many of the sorption sites have a small α and therefore react slowly (see Figure 2). The exact expressions for the first two moments when $a > 1$ are

$$\langle \tau^R(L)\rangle = (1+\beta_{tot})\langle \tau^{NR}(L)\rangle, \quad (30)$$

$$\sigma^{2,R}_{\tau}(L) = \sigma^{2,NR}_{\tau}(L)(1+\beta_{tot})^2 + 2\frac{\beta_{tot}}{b(a-1)}\langle \tau^{NR}(L)\rangle. \quad (31)$$

When $a < 1$, the first moment is still given by (30), but the second moment is infinite. This corresponds to a breakthrough curve with a very long tail. *Haggerty et al.* [2000] have recently demonstrated that under a gamma model, breakthrough curves follow a power law proportional to t^{-a-2}, for large times. Therefore moments of order larger than or equal to $a + 1$ are infinite.

[24] For $a \to \infty$ (while the product ab remains finite) the gamma model converges to the one-site kinetic model. To show this, we make use of the following property of the incomplete gamma function [*Abramowitz and Stegun*, 1974]:

$$\frac{1}{\frac{s}{b}+a+1} < \Big(\frac{s}{b}\Big)^a \exp(s/b)\Gamma(-a,s/b) < \frac{1}{\frac{s}{b}+a}. \quad (32)$$

As $a \gg 1$, the 1 in the denominator of the leftmost term in (32) is negligible, so we can write

$$\Big(\frac{s}{b}\Big)^a \exp(s/b)\Gamma(-a,s/b) \approx \frac{1}{\frac{s}{b}+a}, \quad (33)$$

so that

$$\langle \overline{C}_1(L,s)\rangle = \langle \exp\Big[-s\tau(L)\Big(1+\beta_{tot}\frac{ab}{s+ab}\Big)\Big]\rangle. \quad (34)$$

Equation (34) is formally equivalent to the one-site kinetic equation with $\alpha_1 = ab$. Noticing that ab is precisely the expected value of a gamma distribution with its pdf given by (20), we get that for very large a, the gamma distribution can be replaced with a single mass transfer rate coefficient.

[25] For $a > 1$ and b small, as a increases, the variance of the travel time decreases. This is obvious from (31) because the second term is proportional to $1/(a-1)$. The small value of b causes the second term in (31) to dominate. Physically, when a increases and b is held constant, the mean of the gamma distribution, which is equal to ab, increases. This increase in the reaction rates decreases the kinetic effect so that spreading is reduced. The shape of the travel time variance ratio is the same as for the two-site kinetics model in that it decreases and then becomes constant.

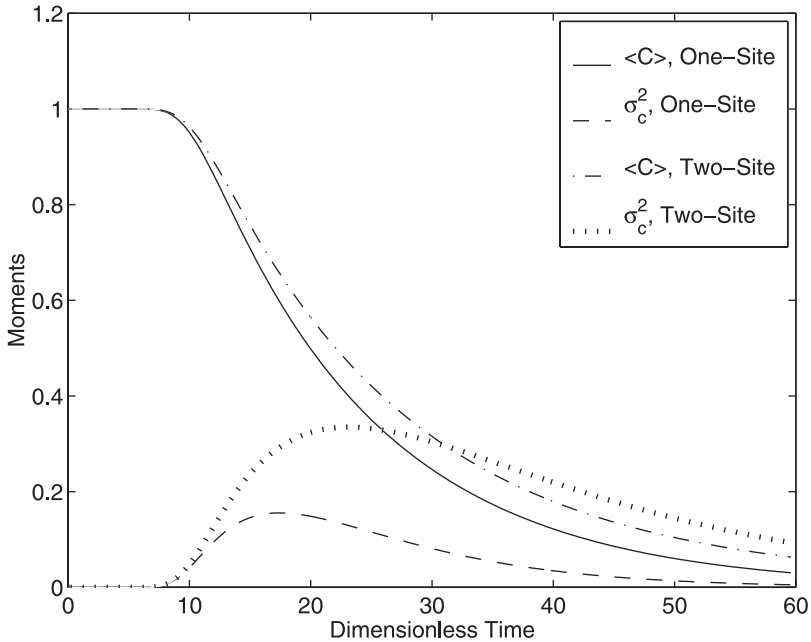

Figure 4. Expected value and variance of the concentration for desorption from an initially contaminated aquifer for a one-site kinetic model with $\beta_{tot} = 1$, $\alpha_1 = 0.1$ and for a two-site kinetics model with $\beta_1 = 0.5$, $\beta_2 = 0.5$, $\alpha_1 = 0.001$, and $\alpha_2 = 0.1$. The dimensionless distance to the control plane, L, is 10 and $\sigma_Y{}^2 = 0.25$.

6.2. Lognormal Model for p(α)

[26] The first temporal moment for the lognormal model is the same as that for the gamma model and is given by (30). The second moment is given by

$$s_t^{2,R}(L) = s_t^{2,NR}(L)(1 + b_{tot})^2 + 2b_{tot}\langle t^{NR}(L)\rangle \exp\left(-\mu + \frac{\sigma^2}{2}\right), \tag{35}$$

and always exists, provided σ is finite.

[27] The ratio of reactive to nonreactive travel time variance for the lognormal model decreases and then becomes constant as shown for the two-site model. As μ, the average of the rate parameters, increases, the variance ratio decreases. This can be understood by noting that as μ increases, the reaction approaches instantaneous equilibrium, which does not produce the spreading that kinetic sorption produces. When the sorption and desorption are kinetic, the ratio of the timescale of desorption to the timescale of advection is larger than when the sorption is instantaneous, so some of the solute plume is advected downstream while the tail is left behind, slowly desorbing. As σ, the standard deviation of the distribution of rate parameters, increases, the variance ratio increases, because when σ is small, most of the sites have a reaction rate parameter near the value of the average, so there is less spreading, as all of the solute experiences a similar reaction.

7. Desorption

[28] Rate-limited desorption from an initially contaminated aquifer by flushing with clean water is an important problem for site remediation, and it has been studied recently in the literature. *Haggerty and Gorelick* [1994] studied different pumping well configurations to remediate a contaminated aquifer governed by a single mass transfer rate coefficient. *Berglund and Cvetkovic* [1995] investigated the effect of several aquifer parameters on the time to cleanup of a contaminant plume for radial flow for the case of a single mass transfer rate coefficient. They found that the time to cleanup increases as the variance of the log hydraulic conductivity increases, and it increases as the mass transfer rate coefficient decreases. Their results also show that an increase in the distribution coefficient causes an increase in the time to cleanup. *Huang and Goltz* [1999] developed analytical results for rate-limited mass transfer in the vadose zone. Our approach can be extended to the case of desorption from an initially contaminated aquifer with an initially uniform mobile concentration, $C_{1,0}$, by changing the initial and boundary conditions.

[29] The initial and boundary conditions are

$$C_1(\eta, T = 0) = C_{1,0}, C_2(\eta, T = 0) = C_{1,0}, \tag{36}$$

$$C_1(\eta \to \infty, T) = C_{1,0} \tag{37}$$

and

$$C_1(\eta = 0, T > 0) = 0. \tag{38}$$

The solution of (2) and (3) for this case is

$$\overline{C}_1(L, s) = \frac{C_{1,0}}{s}\left\{1 - \exp\left[-s\tau(L)\left(1 + \beta_{tot}\int_0^\infty \frac{\alpha p(\alpha)}{s + \alpha} d\alpha\right)\right]\right\}. \tag{39}$$

From the property of the Laplace transform of a derivative, $dC_1(L, t)/dt = s\overline{C}_1(L, s) - C_{1,0}$, it follows that the Laplace transform of the derivative of $-C_1(L, t)/C_{1,0}$ is equal to the

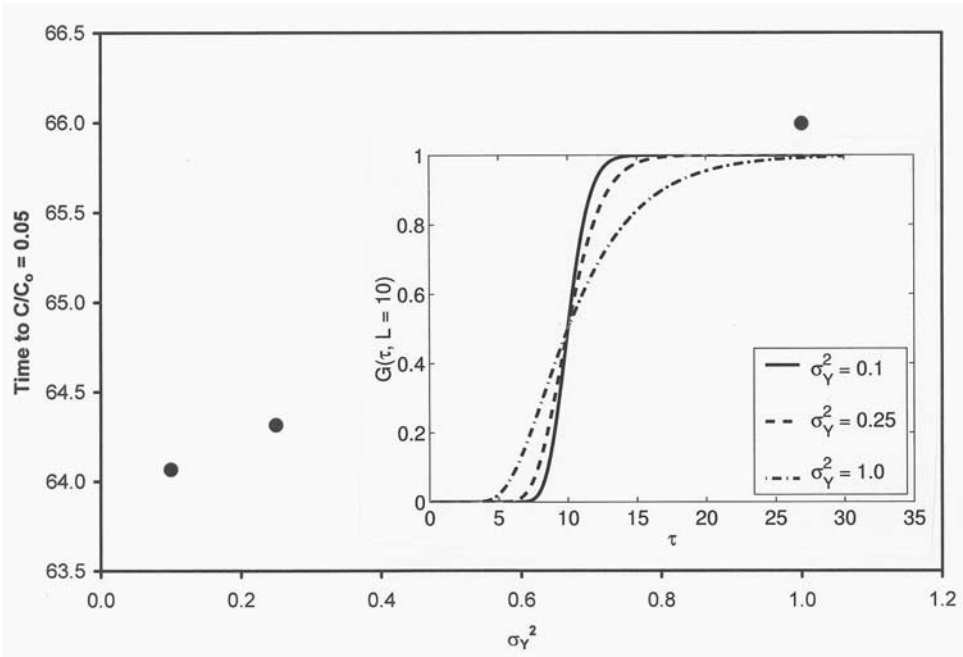

Figure 5. Effect of log hydraulic conductivity variance on the time for an initially contaminated aquifer to be cleaned to 5% of the initial concentration at a plane 10 integral scales downstream. A two-site model was used with $\beta_1 = \beta_2 = 0.5$, $\alpha_1 = 0.001$ and $\alpha_2 = 0.1$. Inset shows CDF of travel time for the same log hydraulic conductivity variances.

right hand side of (10). Therefore expressions similar to (12) apply for the temporal moments of $-dC_1(L, t)/dt$, and the two problems are mathematically very similar.

[30] Figure 4 shows the expected value and variance of the concentration at a control plane 10 integral scales downstream calculated by solving (39) for C(L, t) with a numerical Laplace transform inversion algorithm and using the relationship $\langle C_1^i(L,t)\rangle = \int_0^\infty C_1^i(L,t)g(t,L)dt$ to calculate the moments of the concentration. This gives ensemble moments over many realizations for one streamtube. However, they can also be interpreted as moments over all streamtubes at the control plane when clean water is injected over an infinite plane at L = 0. The geochemical models considered in Figure 4 are a one-site model with $\beta_{tot} = 1$ and $\alpha = 0.1$, and a two-site model with $\beta_1 = 0.5$, $\beta_2 = 0.5$, $\alpha_1 = 0.001$ and $\alpha_2 = 0.1$. The concentration is normalized by the initial concentration. As expected, the normalized expected value of the concentration decreases from one to zero. The variance of the concentration is zero when the normalized expected value of the concentration is stable at one or zero, because no uncertainty in the value of the concentration exists in those cases. The results using the two-site model are similar to those found using the one-site model. However, because α_1 is so much smaller than the α used in the one-site model, which indicates a slower mass transfer rate, the concentration decreases more slowly when the two-site model is used.

[31] The dependence of the time required for flushing of an initially contaminated aquifer with clean water to decrease the concentration at a control plane 10 integral scales downstream on the log hydraulic conductivity variance was investigated. A two-site model was used with $\beta_1 = \beta_2 = 0.5$, $\alpha_1 = 0.001$, and $\alpha_2 = 0.1$. Figure 5 shows the value of the log hydraulic conductivity variance versus the time required for the concentration to decrease to 5% of its original value. As the log hydraulic conductivity variance increases, the time required for cleanup also increases. This is in agreement with the results of *Berglund and Cvetkovic* [1995]. As the log hydraulic conductivity variance increases, the CDF of the travel time becomes more spread out as shown in the inset in Figure 5. Therefore the trailing edge of the contamination is longer, and it takes more time to get to a small percentage of the initial concentration. One would expect that the same phenomena would cause a decrease in the time to reach a large percentage, say 95%, of the initial concentration as the log hydraulic conductivity variance increases. This is indeed the case (results not shown).

8. Conditional Moments

[32] To fully benefit from the measured hydraulic conductivity data, conditioning is often used [*Dagan*, 1989; *Rubin and Dagan*, 1992; *Rubin et al.*, 1999; *Rubin*, 2002]. For our method, nonreactive conditional temporal moments can be used as input. We consider conditioning on all of the available measurements, such as transmissivities, heads, and groundwater flow or velocities, or on soft information, such as geophysical data. Because the chemical parameters are treated as deterministic, randomness is associated only with the travel time. Then, we can immediately write the first two conditional temporal moments as

$$\langle t^R(L)\rangle^C = (1 + b_{tot})\langle t^{NR}(L)\rangle^C, \tag{40}$$

$$s_t^{2,R,C}(L) = s_t^{2,NR,C}(L)(1 + b_{tot})^2 + 2b_{tot}\langle t^{NR}(L)\rangle^C \int_0^\infty \frac{p(a)}{a} da, \tag{41}$$

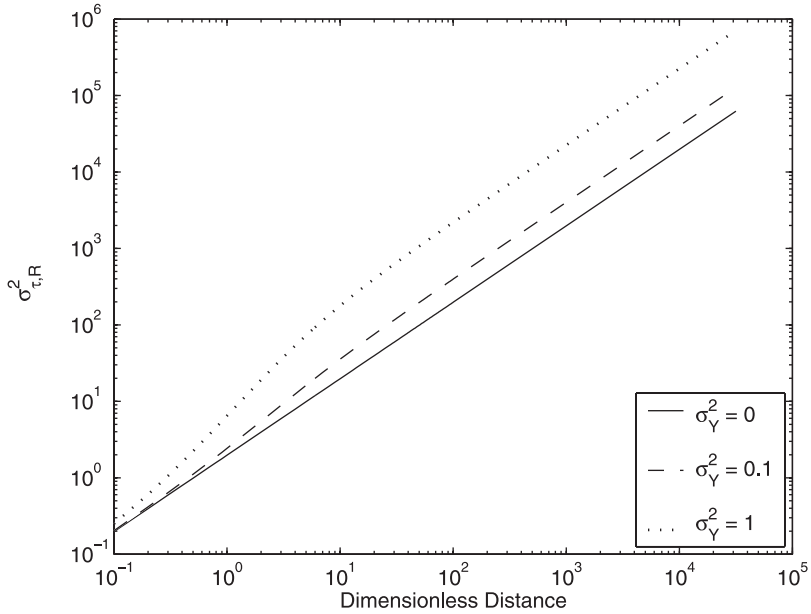

Figure 6. Example showing that travel time variance is not zero when there is no uncertainty in the log hydraulic conductivity. Curves are for a lognormal model with $\beta_{tot} = 2.2$, $\mu = 5.3$, and $\sigma = 3$.

where the superscript C indicates that a moment is conditional. These are ensemble moments and cannot be interpreted as moments over the control plane for one realization, because the measurements make the domain nonstationary. For example, the effect of the measurements on one streamtube is not the same as it is on a streamtube in another location. The conditional CDF of τ, $G^C(L, \tau)$, can be obtained from the unconditional one using Bayesian principles [*Dagan and Nguyen*, 1989; *Rubin and Dagan*, 1992]. One advantage of this type of conditioning is the reduction in uncertainty, which has been demonstrated in several cases [e.g., *Rubin*, 1991; *Harvey and Gorelick*, 1995]. The travel time variance represents both variability between realizations due to uncertainty and actual spread due to kinetic sorption, which is present in even one realization. The first term on the right hand side of equation (41) gives a measure of the uncertainty, while the second term represents the spread caused by kinetic sorption. Figure 6 shows the travel time variance for a lognormal model with $\beta_{tot} = 2.2$, $\mu = 5.3$, and $\sigma = 3$ for different values of the log hydraulic conductivity variance, σ_Y^2. From Figure 6, we see that even when there is no uncertainty in the flow, such as when $\sigma_Y^2 = 0$, the travel time variance is not zero.

[33] We now present examples of the reduction in uncertainty by conditioning. For this purpose, we use numerical results by *Rubin* [1991]. That paper showed several examples of the effect of conditioning with transmissivity values upon statistical moments for nonreactive solutes. In each of the sets, which varied in the amount of conditioning data, the author computed the effect of conditioning on the longitudinal mean displacement, $\langle X_1 \rangle$, and the longitudinal displacement covariance, X_{11}, as a function of travel time. From this information, it is possible to derive the conditional CDF as

$$G^C(L,t) = \frac{1}{2}\mathrm{erfc}\left[\frac{L - < X_1(t) >^C}{\sqrt{2X_{11}^C(t)}}\right]. \qquad (42)$$

We selected two of the examples by *Rubin* [1991] to use here. The first one corresponds to conditioning on 9 transmissivity measurements beginning at the injection point and continuing in the mean flow direction at a spacing of $1.25I_Y$. The value of each measurement was a unit positive fluctuation of the natural logarithm of transmissivity from the mean. The mean and covariance of the longitudinal displacement are given as curve d in Figures 7a and 7b of *Rubin* [1991]. Curve c of Figures 9a and 9b of *Rubin* [1991] shows the mean and covariance of the longitudinal displacement after conditioning on three transmissivity measurements, again with unit positive fluctuations, located at the coordinates (0,1), (5,1), and (10,1), which are nondimensionalized by I_Y. The injection point is at (0,0). We have used these curves to identify the reduction in uncertainty by computing the conditional second reactive temporal moment and comparing it to the unconditional one for a given set of chemical parameters.

[34] The results for four cases of conditioning with the lognormal geochemical model are shown in Figure 7 in terms of the percent reduction of the second moment, computed as

$$\text{Percent Reduction} = \frac{s_t^{2,R,NC}(L) - s_t^{2,R,C}(L)}{s_t^{2,R,NC}(L)} 100\%, \qquad (43)$$

where ^{NC} stands for not conditional. In all cases, the amount of reduction due to conditioning is significant. An important point to make from Figure 7 is that both the shape and the amount of reduction depend strongly on the parameters that define the chemical model. The values of μ and σ used are based on values found by *Haggerty and Gorelick* [1998] and *Culver et al.* [1997] to fit experimental data. Curve a in Figure 7 shows the reduction in the travel time variance for a lognormal model with $\mu = 5.3$ and $\sigma = 3.0$ due to conditioning on the data from Figure 9, curve c, of *Rubin* [1991]. The reduction in travel time variance is around 14%. When larger values for σ ($\sigma = 6.3$ to 10) were used with this

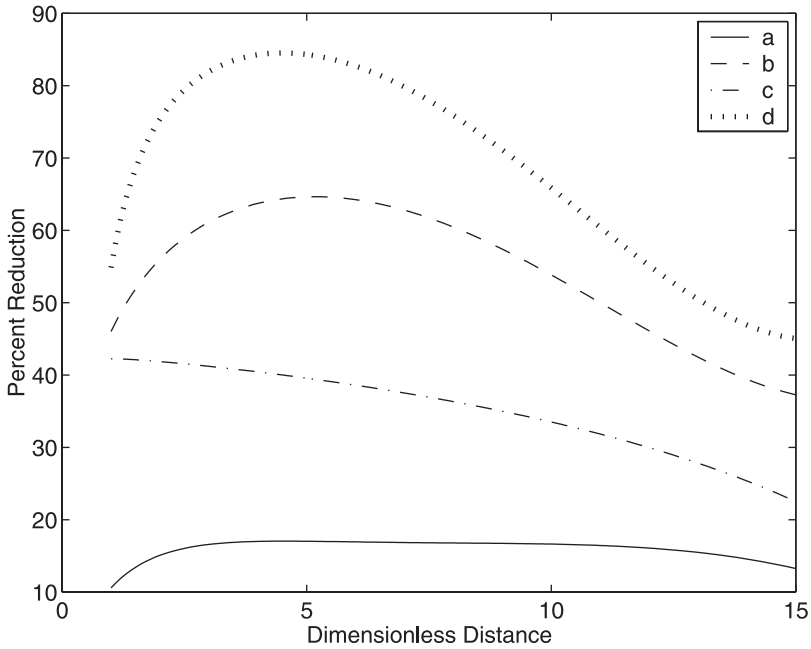

Figure 7. Example of percentage reduction in the conditional variance of travel time with respect to the unconditional one for a reactive solute (equation 43). The chemical model assumed is lognormal with $\beta_{tot} = 2.2$, $\sigma_Y^2 = 0.25$, and $\mu = 5.3$. Curve a shows $\sigma = 3$ and the variance for a tracer is given in Figure 9, curve c, of *Rubin* [1991]. The variance for a tracer for curves b through d is given in Figure 7, curve d, of *Rubin* [1991], and for curve b, $\sigma = 3$; for curve c, $\sigma = 6.3$; and for curve d, $\sigma = 0$.

conditioning data, the reduction was steady at 14% for the entire travel distance analyzed. For the remaining three curves in Figure 7, the set of data from curve d of Figure 7 from *Rubin* [1991] was used, and $\mu = 5.3$. In curve b of Figure 7, $\sigma = 3.0$, and in curve c of Figure 7, $\sigma = 6.3$. For the smaller value of σ, the reduction of variance shows a peak of almost 65% followed by a rapid decline. For the larger value of σ, the reduction of variance is at its maximum of around 42.5% at the shortest distance and gradually reduces at larger distances. This same result is obtained as the value of σ increases. The change in the shape of the curve of the percent reduction in travel time variance with changing values of σ reflects the change from one term of (35) to the other dominating the value of the travel time variance. When σ is small, the first term dominates. Because this term represents the uncertainty, one would expect the conditioning to have a greater impact when the first term dominates. We can see from curve d of Figure 7, that when $\sigma = 0$, the effect of conditioning is even more significant with a maximum variance reduction of almost 85%.

[35] The effect of conditioning decreases with increasing travel distance, because conditioning data only goes up to a distance of 10 integral scales. Some of the curves show an increase in the effectiveness of conditioning with increasing distance while close to the injection point. Very close to the injection point, the solute has not encountered much heterogeneity. There is not much uncertainty, so conditioning is not as effective as it is at slightly later times.

9. Summary and Conclusions

[36] When analyzing solute transport in real field situations, most of the data is in the form of breakthrough curves (BTCs). In a heterogeneous media, the actual shape of the BTC depends on the heterogeneous structure of the domain and on the parameters that characterize the sorptive behavior of the solute. One of the main findings of this paper is that for any chemical model that considers linear mass transfer reactions, it is possible to relate the moments of the BTC to those for a conservative tracer that would be transported in the same medium under the same flow conditions. This is valid for any given realization of the field. Because the moments of the BTC for conservative tracers cannot be obtained exactly (unless measured) in a heterogeneous domain, the moments of the expected BTC are used.

[37] We presented closed form solutions for the continuous diffusion rate model. The method can easily be extended to the multirate models that have been found to fit experimental data in recent literature. We have shown that the method can be applied to the problem of an instantaneous point injection of contaminant and to desorption from an initially contaminated aquifer.

[38] Conditioning is easily addressed in this method. The dependence of the conditional temporal moments on only the chemical parameters and the conditional temporal moments of a nonreactive tracer reduces computational effort, because the moments of the nonreactive tracer can be calculated once, and then used repeatedly with the applicable chemical parameters. We have shown how conditioning can dramatically reduce the variance of travel time. The amount of variance reduction depends on the chemical model selected.

Notation

a shape parameter for the gamma model.
b scale parameter for the gamma model.

C_1 dimensionless mobile concentration.
$C_{1,0}$ dimensionless initial mobile concentration.
C_2 dimensionless immobile concentration.
erfc( ) the complementary error function.
$g(L, \tau)$ probability density function (pdf) of travel time.
$G(L, \tau)$ cumulative distribution function (CDF) of travel time.
I_Y integral scale of the natural log of hydraulic conductivity.
K_D distribution coefficient.
L distance from injection to control plane.
$p(\alpha)$ volumetric fraction of the solid that reacts at a particular rate α.
s Laplace's variable.
T dimensionless time.
$T_i^R(L)$ ith noncentral moment of the expected breakthrough curve.
t real time.
t_i ith noncentral, nonnormalized temporal moment.
U reference velocity.
v velocity.
V dimensionless velocity.
x coordinate along flow direction.
$X_1(\tau)$ longitudinal displacement at time τ.
$X_{11}(\tau)$ longitudinal displacement variance at time τ.
Y natural log of hydraulic conductivity.
α or α_i dimensionless mass transfer rate coefficient.
β_i or $\beta(\alpha)$ capacity coefficient.
β_{tot} total capacity factor.
δ( ) Dirac delta function.
ϕ porosity in the mobile zone.
Γ( ) gamma function.
Γ(,) incomplete gamma function.
η dimensionless coordinate along the stream tube.
μ mean of the natural logarithm of the rate coefficients for the lognormal model.
ρ_s mass density of the soil solids.
σ standard deviation of the distribution of rate coefficients for the lognormal model.
$\sigma_\bullet^2$ variance.
Σ_τ third central moment of travel time.
τ travel time.
C, NC superscripts referring to conditional and not conditional.
R, NR superscripts referring to reactive and nonreactive.

[39] Angle brackets indicate expected value. Overbar indicates Laplace transform.

[40] **Acknowledgments.** Several institutions have provided funding for this research: the National Science Foundation, the Spanish Ministry of Education, and ENRESA.

References

Abramowitz, M., and I. A. Stegun, *Handbook of Mathematical Functions*, 1046 pp., Dover, Mineola, N. Y., 1974.

Aris, R., On the dispersion of linear kinematic waves, *Proc. R. Soc. London, Ser. A*, *245*, 268–277, 1958.

Bellin, A., P. Salandin, and A. Rinaldo, Simulation of dispersion in heterogeneous porous formations-statistics, 1st-order theories, convergence of computations, *Water Resour. Res.*, *28*(9), 2211–2227, 1992.

Berglund, S., and V. Cvetkovic, Pump-and-treat remediation of heterogeneous aquifers: Effects of rate-limited mass transfer, *Ground Water*, *33*(4), 675–685, 1995.

Buchan, G. D., K. S. Grewal, and A. B. Robson, Improved models of particle-size distribution: An illustration of model comparison techniques, *Soil Sci. Soc.*, *57*, 901–908, 1993.

Chen, W. L., and R. J. Wagenet, Solute transport in porous media with sorption-site heterogeneity, *Environ. Sci. Technol.*, *29*(11), 2725–2734, 1995.

Connaughton, D. F., J. R. Stedinger, L. W. Lion, and M. L. Shuler, Description of time-varying desorption kinetics: Release of naphthalene from contaminated soils, *Environ. Sci. Technol.*, *27*(12), 2397–2403, 1993.

Culver, T. B., S. P. Hallisey, D. Sahoo, J. J. Deitsh, and J. A. Smith, Modeling the desorption of organic contaminants from long-term contaminated soil using distributed mass transfer rates, *Environ. Sci. Technol.*, *31*(6), 1581–1588, 1997.

Cvetkovic, V. D., and A. M. Shapiro, Mass arrival of sorptive solute in heterogeneous porous media, *Water Resour. Res.*, *26*(9), 2057–2067, 1990.

Cvetkovic, V., A. M. Shapiro, and G. Dagan, A solute flux approach to transport in heterogeneous formations, 2, Uncertainty analysis, *Water Resour. Res.*, *28*(5), 1377–1388, 1992.

Cvetkovic, V., H. Cheng, and X.-H. Wen, Analysis of nonlinear effects on tracer migration in heterogeneous aquifers using Lagrangian travel time statistics, *Water Resour. Res.*, *32*(6), 1671–1680, 1996.

Cvetkovic, V., G. Dagan, and H. Cheng, Contaminant transport in aquifers with spatially variable hydraulic and sorption properties, *Proc. R. Soc. London, Ser. A*, *454*, 2173–2207, 1998.

Cvetkovic, V., J. O. Selroos, and H. Cheng, Transport of reactive tracers in rock fractures, *J. Fluid Mech.*, *378*, 335–356, 1999.

Dagan, G., *Flow and Transport in Porous Formations*, 465 pp., Springer-Verlag, New York, 1989.

Dagan, G., and P. Indelman, Reactive solute transport in flow between a recharging and a pumping well in a heterogeneous aquifer, *Water Resour. Res.*, *35*(12), 3639–3647, 1999.

Dagan, G., and V. Nguyen, A comparison of travel time and concentration approaches to modeling transport by groundwater, *J. Contam. Hydrol.*, *4*, 79–91, 1989.

Deitsch, J. J., J. A. Smith, T. B. Culver, R. A. Brown, and S. A. Riddle, Distributed-rate model analysis of 1,2-dichlorobenzene batch sorption and desorption rates for five natural sorbents, *Environ. Sci. Technol.*, *34*(8), 1469–1476, 2000.

Goltz, M. N., and P. V. Roberts, Using the method of moments to analyze three-dimensional diffusion-limited solute transport from temporal and spatial perspectives, *Water Resour. Res.*, *23*(8), 1575–1585, 1987.

Grathwohl, P., *Diffusion in Natural Porous Media: Contaminant Transport, Sorption/Desorption and Dissolution Kinetics*, 207 pp., Kluwer Acad., Norwell, Mass., 1998.

Haggerty, R., and S. M. Gorelick, Design of multiple contaminant remediation: Sensitivity to rate-limited mass transfer, *Water Resour. Res.*, *30*(2), 435–446, 1994.

Haggerty, R., and S. M. Gorelick, Multiple-rate mass transfer for modeling diffusion and surface reactions in media with pore-scale heterogeneity, *Water Resour. Res.*, *31*(10), 2383–2400, 1995.

Haggerty, R., and S. M. Gorelick, Modeling mass transfer processes in soil columns with pore-scale heterogeneity, *Soil Sci. Soc. Am. J.*, *62*, 62–74, 1998.

Haggerty, R., S. A. McKenna, and L. C. Meigs, On the late-time behavior of tracer test breakthrough curves, *Water Resour. Res.*, *36*(12), 3467–3479, 2000.

Haggerty, R., S. W. Fleming, L. C. Meigs, and S. A. McKenna, Tracer tests in a fractured dolomite, 2, Analysis of mass transfer in single-well injection-withdrawal tests, *Water Resour. Res.*, *37*(5), 1129–1142, 2001.

Harvey, C. F., and S. M. Gorelick, Temporal moment-generating equations: Modeling transport and mass transfer in heterogeneous aquifers, *Water Resour. Res.*, *31*(8), 1895–1911, 1995.

Huang, J., and M. N. Goltz, Solutions to equations incorporating the effect of rate-limited contaminant mass transfer on vadose zone remediation by soil vapor extraction, *Water Resour. Res.*, *35*(3), 879–883, 1999. (Correction, *Water Resour. Res.*, *36*(11), 3389, 2000.)

James, A. I., W. D. Graham, K. Hatfield, P. S. C. Rao, and M. D. Annable, Optimal estimation of residual non-aqueous phase liquid saturations using partitioning tracer concentration data, *Water Resour. Res.*, *33*(12), 2621–2636, 1997.

Karapanagioti, H. K., D. A. Sabatini, S. Kleineidam, P. Grathwohl, and B. Ligouis, Phenanthrene sorption with heterogeneous organic matter

in a landfill aquifer material, *Phys. Chem. Earth*, *24*(6), 535–541, 1999.

McKenna, S. A., L. C. Meigs, and R. Haggerty, Tracer tests in a fractured dolomite, 3, Double-porosity, multiple-rate mass transfer processes in convergent flow tracer tests, *Water Resour. Res.*, *37*(5), 1143–1154, 2001.

Pedit, J. A., and C. T. Miller, Heterogeneous sorption processes in subsurface systems, 1, Model formulations and applications, *Environ. Sci. Technol.*, *28*(12), 2094–2104, 1994.

Rubin, Y., Prediction of tracer plume migration in disordered porous media by the method of conditional probabilities, *Water Resour. Res.*, *27*(6), 1291–1308, 1991.

Rubin, Y., *Applied Stochastic Hydrogeology*, Oxford Univ. Press, New York, in press, 2002.

Rubin, Y., and G. Dagan, Conditional estimation of solute travel time in heterogeneous formations: Impact of transmissivity measurements, *Water Resour. Res.*, *28*(4), 1033–1040, 1992.

Rubin, Y., M. A. Cushey, and A. Wilson, The moments of the breakthrough curves of instantaneously and kinetically sorbing solutes in heterogeneous geologic media: Prediction and parameter inference from field measurements, *Water Resour. Res.*, *33*(11), 2465–2481, 1997.

Rubin, Y., A. Sun, R. Maxwell, and A. Bellin, The concept of block-effective macrodispersivity and a unified approach for grid-scale- and plume-scale-dependent transport, *J. Fluid Mech.*, *395*, 161–180, 1999.

Sanchez-Vila, X., On the geostatistical formulations of the groundwater flow and solute transport equations, Ph.D. thesis, Univ. Politec. de Catalunya, Barcelona, Spain, 1995.

Selroos, J. O., Temporal moments for nonergodic solute transport in heterogeneous aquifers, *Water Resour. Res.*, *31*(7), 1705–1712, 1995.

Selroos, J. O., and V. Cvetkovic, Modeling solute advection coupled with sorption kinetics in heterogeneous formations, *Water Resour. Res.*, *28*(5), 1271–1278, 1992.

Shapiro, A. M., and V. D. Cvetkovic, Stochastic analysis of solute arrival time in heterogeneous porous media, *Water Resour. Res.*, *24*(10), 1711–1718, 1988.

Valocchi, A. J., Validity of the local equilibrium assumption for modeling sorbing solute transport through homogeneous soils, *Water Resour. Res.*, *21*(6), 808–820, 1985.

van Genuchten, M. T., and P. J. Wierenga, Numerical solution for convective dispersion with intra-aggregate diffusion and non-linear adsorption, in *Proceedings of the IFIP Working Conference on Biosystems Simulation in Water Resources and Waste Problems*, edited by G. C. Vansteenkiste, pp. 275–292, North-Holland, New York, 1976.

A. E. Lawrence and Y. Rubin, Department of Civil and Environmental Engineering, University of California, Berkeley, CA 94720, USA. (rubin@ce.berkeley.edu)

X. Sanchez-Vila, Department of Geotechnical Engineering and Geosciences, Technical University of Catalonia, 08034 Barcelona, Spain.